



Activation of COX-2/PGE₂ Promotes Sapovirus Replication via the Inhibition of Nitric Oxide Production

Mia Madel Alfajaro,^a Jong-Soon Choi,^b Deok-Song Kim,^d Ja-Young Seo,^a Ji-Yun Kim,^a Jun-Gyu Park,^a Mahmoud Soliman,^a Yeong-Bin Baek,^a Eun-Hyo Cho,^a Joseph Kwon,^b Hyung-Jun Kwon,^c Su-Jin Park,^c Woo Song Lee,^c Mun-Il Kang,^a Myra Hosmillo,^d Ian Goodfellow,^d Kyoung-Oh Cho^a

Laboratory of Veterinary Pathology, College of Veterinary Medicine, Chonnam National University, Gwangju, Republic of Korea^a; Division of Life Science, Korea Basic Science Institute, Seoul, Republic of Korea^b; Bioindustry Research Center, Korea Research Institute of Bioscience and Biotechnology, Daejeon, Republic of Korea^c; Division of Virology, Department of Pathology, University of Cambridge, Cambridge, United Kingdom^d

ABSTRACT Enteric caliciviruses in the genera *Norovirus* and *Sapovirus* are important pathogens that cause severe acute gastroenteritis in both humans and animals. Cyclooxygenases (COXs) and their final product, prostaglandin E₂ (PGE₂), are known to play important roles in the modulation of both the host response to infection and the replicative cycles of several viruses. However, the precise mechanism(s) by which the COX/PGE₂ pathway regulates sapovirus replication remains largely unknown. In this study, infection with porcine sapovirus (PSaV) strain Cowden, the only cultivable virus within the genus *Sapovirus*, markedly increased COX-2 mRNA and protein levels at 24 and 36 h postinfection (hpi), with only a transient increase in COX-1 levels seen at 24 hpi. The treatment of cells with pharmacological inhibitors, such as non-steroidal anti-inflammatory drugs or small interfering RNAs (siRNAs) against COX-1 and COX-2, significantly reduced PGE₂ production, as well as PSaV replication. Expression of the viral proteins VPg and ProPol was associated with activation of the COX/PGE₂ pathway. We observed that pharmacological inhibition of COX-2 dramatically increased NO production, causing a reduction in PSaV replication that could be restored by inhibition of nitric oxide synthase via the inhibitor *N*-nitro-L-methyl-arginine ester. This study identified a pivotal role for the COX/PGE₂ pathway in the regulation of NO production during the sapovirus life cycle, providing new insights into the life cycle of this poorly characterized family of viruses. Our findings also reveal potential new targets for treatment of sapovirus infection.

IMPORTANCE Sapoviruses are among the major etiological agents of acute gastroenteritis in both humans and animals, but little is known about sapovirus host factor requirements. Here, using only cultivable porcine sapovirus (PSaV) strain Cowden, we demonstrate that PSaV induced the vitalization of the cyclooxygenase (COX) and prostaglandin E₂ (PGE₂) pathway. Targeting of COX-1/2 using nonsteroidal anti-inflammatory drugs (NSAIDs) such as the COX-1/2 inhibitor indomethacin and the COX-2-specific inhibitors NS-398 and celecoxib or siRNAs targeting COXs, inhibited PSaV replication. Expression of the viral proteins VPg and ProPol was associated with activation of the COX/PGE₂ pathway. We further demonstrate that the production of PGE₂ provides a protective effect against the antiviral effector mechanism of nitric oxide. Our findings uncover a new mechanism by which PSaV manipulates the host cell to provide an environment suitable for efficient viral growth, which in turn can be a new target for treatment of sapovirus infection.

KEYWORDS caliciviruses, cyclooxygenases, nitric oxide, prostaglandin E₂, sapovirus

Received 28 August 2016 Accepted 15 November 2016

Accepted manuscript posted online 23 November 2016

Citation Alfajaro MM, Choi J-S, Kim D-S, Seo J-Y, Kim J-Y, Park J-G, Soliman M, Baek Y-B, Cho E-H, Kwon J, Kwon H-J, Park S-J, Lee WS, Kang M-I, Hosmillo M, Goodfellow I, Cho K-O. 2017. Activation of COX-2/PGE₂ promotes sapovirus replication via the inhibition of nitric oxide production. *J Virol* 91:e01656-16. <https://doi.org/10.1128/JVI.01656-16>.

Editor Susana López, Instituto de Biotecnología/UNAM

Copyright © 2017 Alfajaro et al. This is an open-access article distributed under the terms of the Creative Commons Attribution 4.0 International license.

Address correspondence to Ian Goodfellow, ig299@cam.ac.uk, or Kyoung-Oh Cho, choko@chonnam.ac.kr.

M.M.A. and J.-S.C. contributed equally to this paper.

Diarrhea is the second greatest cause of mortality in children worldwide (1). Viruses within the genera *Norovirus* and *Sapovirus* in the family *Caliciviridae* are significant causes of gastroenteritis in humans and animals, with noroviruses alone causing ~200,000 deaths per annum in children <5 years of age (2, 3). Despite their socio-economic impact, the fastidious nature of viruses within these genera has significantly hindered our understanding of their life cycles and the development of vaccines and therapeutics (4, 5). Porcine sapovirus (PSaV) is the only cultivable member of the genus *Sapovirus* and replicates in the presence of porcine intestinal contents or bile acids (4, 5). Therefore, PSaV serves as a robust model for studies on the sapovirus life cycle and for the development of therapeutic interventions (6).

The coexistence of viruses and their hosts imposes evolutionary pressure on both the virus and the host immune system. Therefore, viruses have evolved diverse strategies to create a suitable environment conducive to their existence by either activating or suppressing cellular pathways to facilitate replication. The cyclooxygenase-2 (COX-2)/prostaglandin E₂ (PGE₂) pathway is one of several host pathways that participate in the modulation of the host response to the infection and the replicative life cycle of viruses (7). For example, the activation of the COX-2/PGE₂ pathway results in increased replication of cytomegalovirus (8, 9), but PGE₂ inhibits the replication of parainfluenza 3 virus and adenovirus (10, 11). COXs convert arachidonic acid released by phospholipase A₂- and C-mediated hydrolysis of plasma membrane phospholipids following exposure to diverse physiological and pathological stimuli into prostaglandins (PGs), prostacyclins, and thromboxanes (12, 13). Three forms of COX have been identified to date, with COX-1 and COX-2 the most widely studied. COX-1 is constitutively expressed and is known to synthesize various PGs, including PGE₂, that participate in a diverse range of normal physiological processes, such as cytoprotection of the gastric mucosa, regulation of renal blood flow, bone metabolism, nerve growth and development, wound healing, and platelet aggregation (12, 13). In contrast, COX-2 is rapidly induced by various stimuli, including viral infection, and catalyzes the synthesis of various PGs, including PGE₂, that have varied activities, including proangiogenic or antiapoptotic properties (12, 13). Some of the biological effects of PGE₂ on immunity and inflammation are exerted through binding to G-protein-coupled receptors on the plasma membrane called E prostanoid receptors (14). PGE₂ is recognized as the major prostanoid produced in immune and nonimmune cells and acts as a potent regulator of cell-cell interaction, antigen presentation, cytokine production, differentiation, survival, apoptosis, and cell migration (14).

This study examines the potential role of the COX/PGE₂ pathway in the regulation of the sapovirus life cycle. We demonstrate that the COX/PGE₂ pathway is induced during PSaV replication and that this induction occurs following the expression of the viral VPg and protease-polymerase (ProPol) proteins. We further demonstrate that the production of PGE₂ provides a protective effect against the antiviral effector mechanism of nitric oxide (NO), uncovering a new mechanism by which enteropathogenic viruses manipulate the host cell to provide an environment suitable for efficient viral growth.

RESULTS

PSaV infection induces COX expression and leads to the production of PGE₂. To determine whether the COX/PGE₂ pathway is activated during PSaV replication, we examined the impact of PSaV replication on COX gene expression. COX-2 mRNA and protein levels were markedly elevated at 24 and 36 h postinfection (hpi), concomitant with the increase in PSaV viral RNA and protein levels, whereas COX-1 levels were transiently increased at 24 hpi only (Fig. 1A to C). The level of PGE₂ in the infected cell culture supernatant was also significantly elevated from 12 hpi (Fig. 1D).

To confirm whether the observed increase in soluble PGE₂ was a direct result of the PSaV-mediated induction of COX-1 and COX-2, the effect of selective or nonselective COX inhibitors on PGE₂ production was examined (Fig. 2). Importantly, all the studies were performed at doses of inhibitors shown not to affect cell viability under the

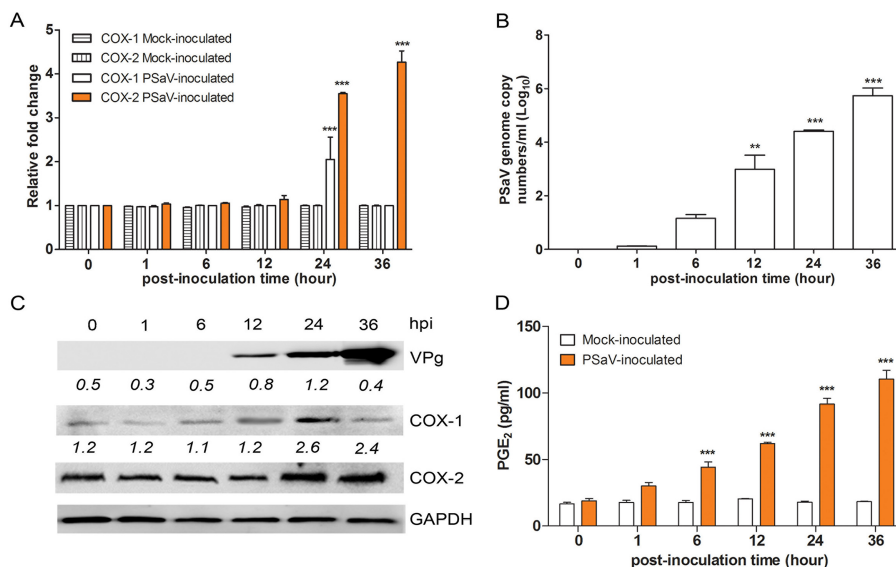


FIG 1 Induction of COX-1 and COX-2 by PSaV infection. (A and B) The expression of COX-1, COX-2, and PSaV viral RNA in LLC-PK cells infected with PSaV (MOI = 1 FFU/cell) was quantified by real-time PCR (qPCR). In the cases of COX-1 and COX-2, expression levels were normalized to β -actin and are depicted as the fold induction compared with that of the mock-inoculated cells. (C) The levels of the VPg, COX-1, COX-2, and GAPDH proteins were analyzed by Western blotting. GAPDH was used as a loading control. (D) The levels of PGE₂ in the supernatants harvested at 36 hpi from PSaV-infected LLC-PK cells were determined by ELISA. The levels of PGE₂ in the supernatants were compared between mock- and virus-inoculated groups. The data are presented as means and standard errors of the mean from the results of three independent experiments. Differences were evaluated using one-way analysis of variance (ANOVA). **, $P < 0.001$; ***, $P < 0.0001$.

experimental conditions used (data not shown). The nonselective COX-1/2 inhibitor indomethacin and the selective COX-2 inhibitor NS-398 both inhibited PSaV-mediated PGE₂ production in a dose-dependent manner when added either immediately after the removal of the virus inoculum (posttreatment) or during the entire course of the infection (pre/posttreatment) (Fig. 2A and B). In contrast, due to the reversible nature of the inhibitors, the pretreatment of cells and subsequent removal of the inhibitor prior to the addition of PSaV had no effect on the levels of PGE₂ production (Fig. 2A and B). Similar results were also obtained with a range of other COX inhibitors (Fig. 2C and D and data not shown).

To further confirm direct roles for COX-1 and COX-2 in the production of PGE₂ during PSaV infection, the effects of COX-1- or COX-2-specific small interfering RNAs (siRNAs) were also examined. Transfection of siRNA against COX-1 or COX-2 into LLC-PK cells reduced the expression levels of their respective target proteins. Although the inhibition of both intracellular proteins by siRNA transfection was not complete, the levels of PGE₂ released from COX-1 and COX-2 siRNA-transfected cells were significantly reduced (Fig. 2E and F). These results confirmed that the induction of both COX enzymes was responsible for the observed increase in PGE₂ from PSaV-infected cells. In addition, the level of siRNA-mediated reduction of COX-1 and COX-2 was sufficient to significantly reduce the production of PGE₂.

Inhibition of both COX enzymes negatively regulates PSaV replication. To determine the impact of COX induction on PSaV replication, we examined the effects of COX inhibitors and siRNAs on PSaV replication. Cells were either treated with inhibitors (selective or nonselective) or transfected with siRNAs specific for COX-1 or COX-2, and the effect on virus replication was monitored at 36 hpi by examining viral titers, as well as viral RNA and protein levels. There was no significant effect of COX inhibitors on PSaV replication when cells were pretreated but the inhibitors were removed prior to infection (pretreatment) (Fig. 3A to H and 4A to D). However, the inclusion of COX inhibitors following the removal of the virus inoculum (posttreatment)

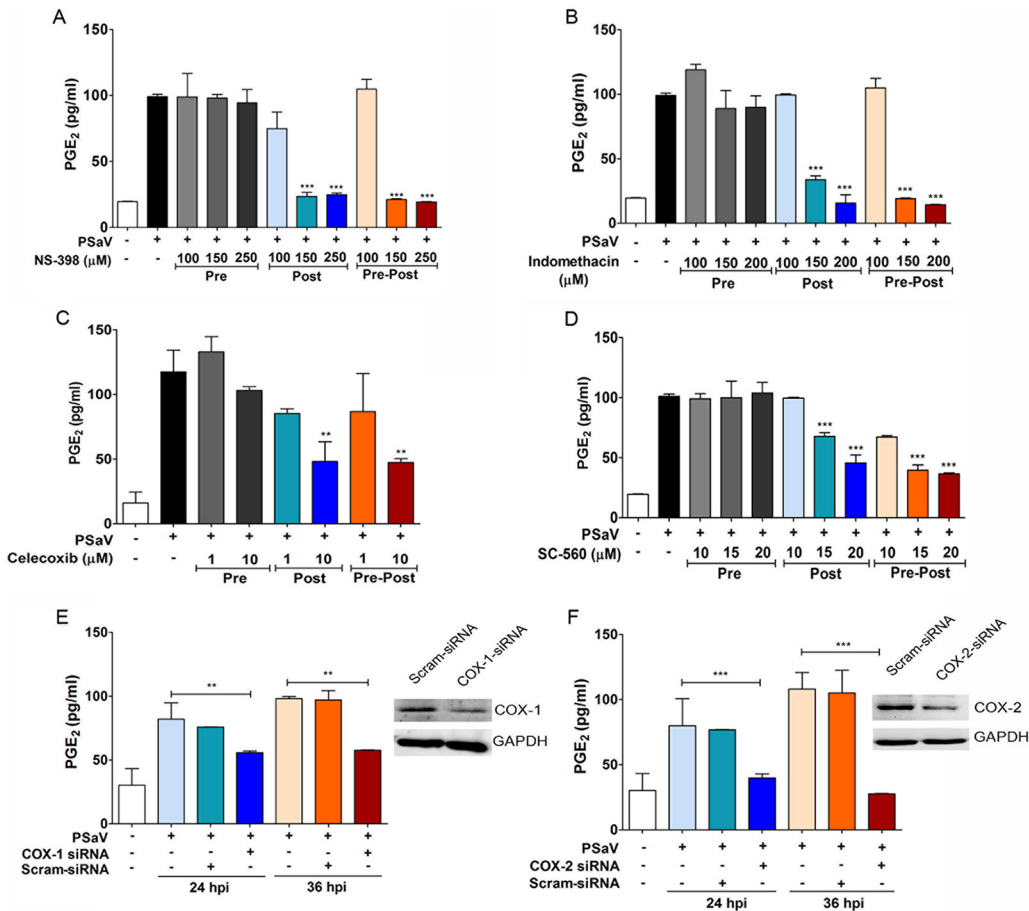


FIG 2 Effects of COX-2 inhibitors on PGE₂ production during PSaV infection. (A to D) LLC-PK cells were treated with selective COX-2 inhibitors (NS398 and celecoxib), a nonselective COX inhibitor (indomethacin), and a selective COX-1 inhibitor (SC-560) as indicated prior to the addition of the virus inoculum (MOI = 1 FFU/cell), and then the inhibitor(s) was removed (Pre); after the addition of the virus inoculum, and then the inhibitor(s) was left for the duration of the infection (Post); or prior to the addition of the inoculum, as well as for the duration of the infection (Pre-Post). The levels of PGE₂ in the supernatants harvested at 36 hpi were determined by ELISA. The levels of PGE₂ in the supernatants of virus-infected cultures were compared between the mock- and chemical-treated groups. (E and F) Confluent LLC-PK cells were transfected with siRNAs against COX-1, COX-2, or scrambled siRNA (Scram-siRNA) prior to infection with PSaV (MOI = 1 FFU/cell). The supernatants were collected, and ELISA was conducted to determine the PGE₂ concentrations. The levels of PGE₂ in the supernatants were compared between mock- and siRNA-transfected groups. (Insets) Western blot analysis for COX-1, COX-2, and GAPDH was conducted with LLC-PK cells transfected with COX-1, COX-2, or scrambled siRNA. The data are presented as means and standard errors of the mean from the results of three independent experiments. Differences were evaluated using one-way ANOVA. **, *P* < 0.001; ***, *P* < 0.0001.

or during the entire course of infection (pre/posttreatment) resulted in a significant reduction in PSaV replication (Fig. 3A to H and 4A to D). The COX-1 inhibitor SC-560 reduced the levels of PSaV RNA and infectious virus by up to ~10-fold at 36 hpi (Fig. 3G to H). In contrast, the COX-2-specific inhibitors NS-398 and celecoxib and the nonselective COX-1/2 inhibitor indomethacin showed more significant effects, typically leading to an ~1,000-fold decrease in virus yield and RNA synthesis (Fig. 3A to F). Other COX-2-specific inhibitors (SC-58125, SC-236, and nimesulide) were also tested; however, less robust inhibition of PSaV replication was observed (data not shown).

The effects of COX-specific siRNAs on PSaV replication were also examined (Fig. 3I to L and 4E and F). Transfection of COX-2-specific siRNA had a more substantial effect on PSaV replication than that of COX-1 siRNAs, causing an ~1,000-fold reduction in the viral titer with a concomitant decrease in viral RNA levels and viral protein production (Fig. 4E and F). Infection assays also demonstrated that either treatment of cells with NS-398 or transfection with COX-2-specific siRNAs resulted in a significant decrease in the number PSaV antigen-positive cells (Fig. 4G). Combined, these data suggest that

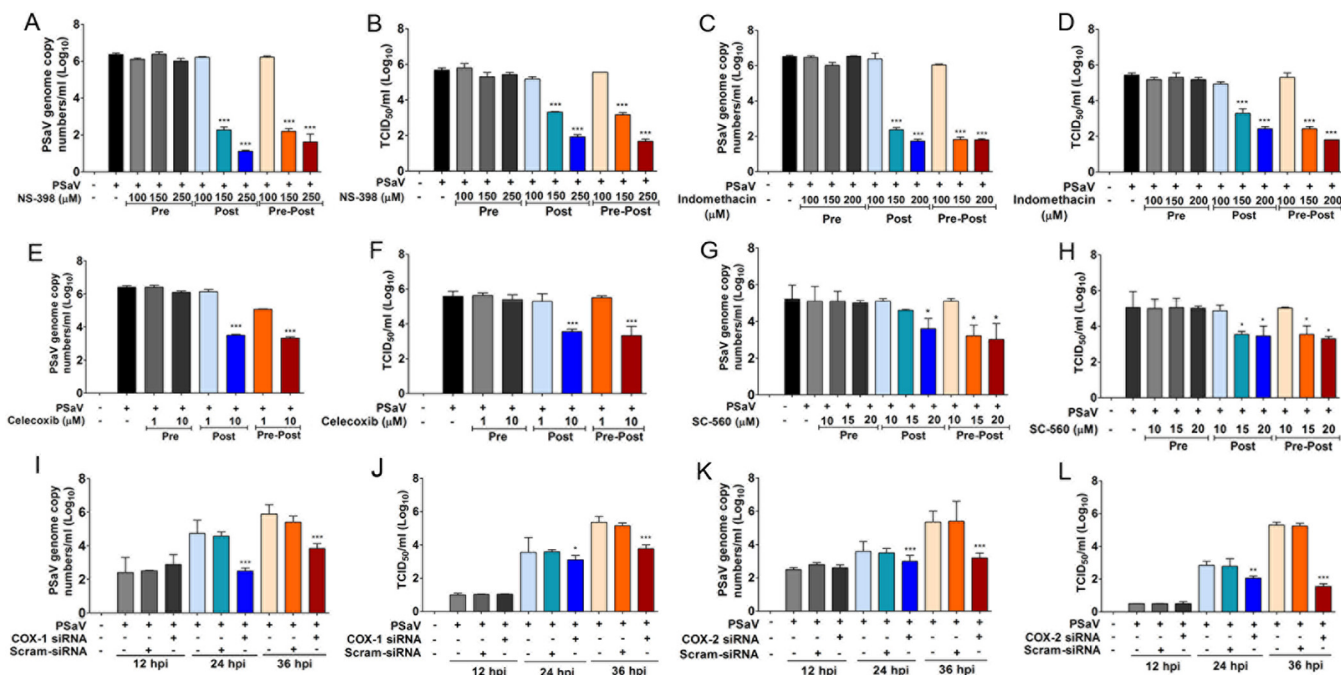


FIG 3 Inhibition of COXs attenuates PSaV replication. (A to H) LLC-PK cells were pretreated (Pre), posttreated (Post), or pre/posttreated (Pre-Post) with nontoxic doses of NS-398, indomethacin, celecoxib, and SC560. At 36 hpi with PSaV (MOI = 1 FFU/cell), cells were harvested, and the levels of viral RNA (A, C, E, and G) and the titer (B, D, F, and H) were determined by quantitative real-time PCR and TCID₅₀, respectively. (I to L) LLC-PK cells were transfected with siRNAs against COX-1, COX-2, or scrambled siRNA before inoculation with PSaV (MOI = 1 FFU/cell). Samples were harvested at 36 hpi, and the levels of viral RNA (I and K) and the titer (J and L) were determined by quantitative real-time PCR and TCID₅₀, respectively. The data are displayed as means and standard errors of the mean from the results of three independent experiments. Differences were evaluated using one-way ANOVA. *, *P* < 0.05; **, *P* < 0.001; ***, *P* < 0.0001.

both COX-1 and COX-2 enhance PSaV replication, possibly via the increased production of PGE₂.

Supplementation of PGE₂ relieves COX inhibition of PSaV replication. If the proviral effect of COX gene induction on PSaV replication was due solely to the production of increased PGE₂, then the addition of PGE₂ would be expected to reverse the inhibitory effect of COX inhibitors on virus replication. To examine this possibility, the ability of exogenous PGE₂ to restore PSaV replication after treatment with the nonselective COX-1/2 inhibitor indomethacin and the COX-2-specific inhibitor NS-398 was examined. The addition of exogenous PGE₂ led to a dose-dependent restoration of both PSaV infectivity and viral RNA levels in cells treated with either inhibitor (Fig. 5). These results confirmed that PGE₂, the final product of both COX enzymes, mediates the proviral effects of COX gene induction on PSaV replication.

Bile acid does not influence COX-2 expression during PSaV infection. PSaV replication in cell culture relies on the presence of bile acids, including glycochenodeoxycholic acid (GCDCA), in the cell culture medium through a function that had previously been linked to an effect of bile acids on the innate immune response to infection (15). However, recent studies have indicated that this initial conclusion was incorrect, as PSaV remains sensitive to the type I interferon (IFN) response in the presence of bile acids (6) and bile acids function to promote virus uncoating (16). To determine whether bile acids have an effect on the induction of the COX-2/PGE₂ pathway during PSaV replication, the induction of COX-2 and PGE₂ was examined in the presence or absence of GCDCA following the transfection of the *in vitro*-transcribed and capped PSaV genome (Fig. 6). Transfected RNA was used to bypass any role of GCDCA during viral entry and uncoating (16). We observed that COX-2 and PGE₂ were induced in cells transfected with *in vitro*-transcribed and capped PSaV genomic RNA, irrespective of whether GCDCA was present or absent (Fig. 6A). As expected, the COX-2 inhibitor NS-398 reduced expression of COX-2 and PGE₂ and replication of PSaV (Fig. 6A

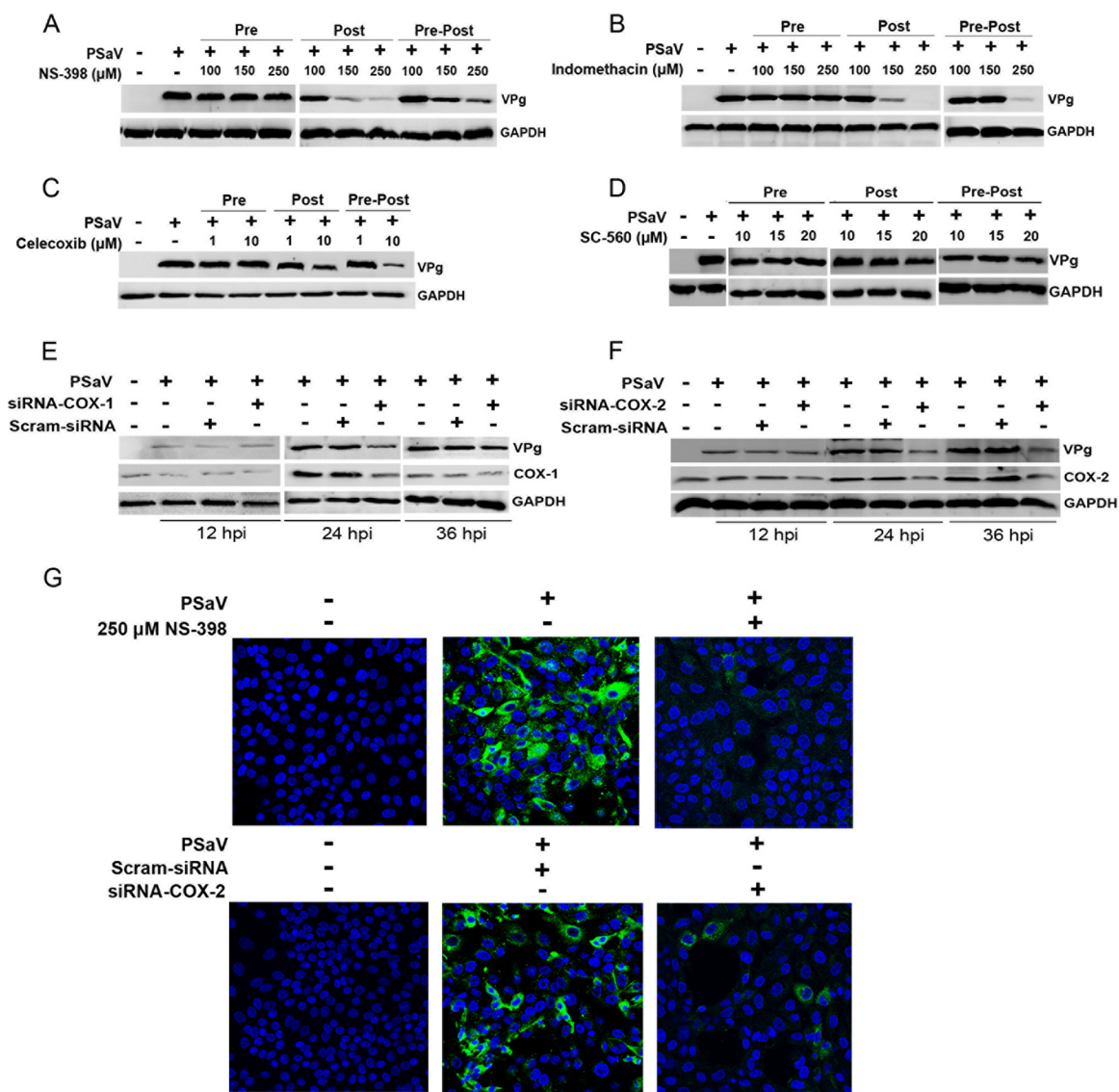


FIG 4 Effects of COX inhibitors or siRNA on PSaV replication. (A to D) LLC-PK cells were pretreated (Pre), posttreated (Post), or pre/posttreated (Pre-Post) with noncytotoxic doses of NS-398, indomethacin, celecoxib, and SC560. At 36 hpi with PSaV (MOI = 1 FFU/cell), cells were harvested, and the levels of viral VPg were determined by Western blot analyses. (E and F) LLC-PK cells were transfected with siRNAs against COX-1, COX-2, or scrambled siRNA before inoculation with PSaV (MOI = 1 FFU/cell). Samples were harvested and processed as described above. GAPDH was used as a loading control. (G) LLC-PK cells were infected with PSaV (MOI = 1 FFU/cell), and the effect of the COX-2 inhibitor NS-398 on viral antigen production was determined by confocal microscopy.

to D). These data indicate that induction of COX-2 and PGE₂ was a direct result of PSaV replication and was not due to any supplementary effect of GCDCA.

PSaV VPg and ProPol activate the COX-2/PGE₂ pathway. Given our observation that PSaV replication was required for the induction of the COX-2/PGE₂ pathway, we investigated whether the expression of viral protein alone was sufficient. LLC-PK cells were transfected with plasmids carrying each PSaV gene, including the NS1, NS2, NS3, NS4, NS5, NS6-7, VP1, and VP2 genes (17). Expression of each viral protein was confirmed via the detection of a hemagglutinin (HA) tag fused to the N terminus of each protein (Fig. 7A). Western blotting and quantitative-PCR (qPCR) analysis of the levels of COX-1 and COX-2 demonstrated that VPg or ProPol expression significantly enhanced the expression of COX-2 and led to an increase in PGE₂ production (Fig. 7B to D).

PGE₂ blocks the antiviral effect of NO. Previous studies have indicated that at least one of the effects of prostaglandin production is the regulation of NO production

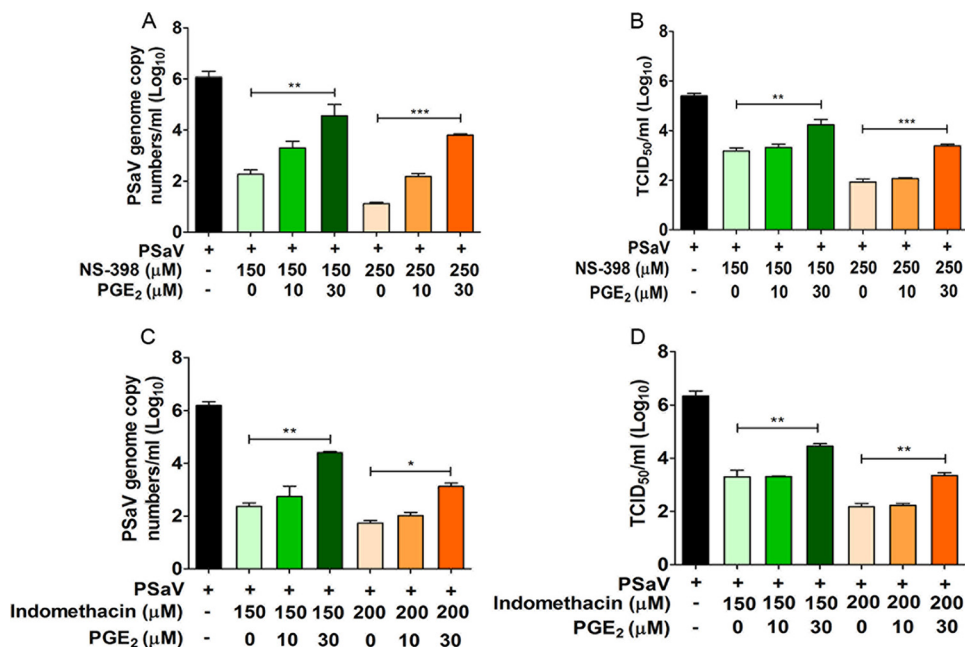


FIG 5 Addition of exogenous PGE₂ reverses the effects of COX inhibitors on PSaV replication. LLC-PK cells were infected with PSaV (MOI = 1 FFU/cell), treated with nontoxic doses of NS-398 or indomethacin, and then supplemented with exogenous PGE₂ in the maintenance medium. After 36 h postinfection, cells were harvested, and the levels of viral RNA synthesis (A and C) and the titer (B and D) were determined by quantitative real-time PCR and TCID₅₀, respectively. The data are represented as means and standard errors of the mean from the results of three independent experiments. Differences were evaluated using one-way ANOVA. *, *P* < 0.05; **, *P* < 0.001; ***, *P* < 0.001.

(18). NO is a key molecule involved in the host defense mechanism against various pathogens, including protozoans, parasites, fungi, bacteria, and viruses (19). NO also has a regulatory role at many stages of the development of inflammation (20). To determine if the PGE₂ produced during PSaV replication impacted NO production, we first examined the level of NO produced during PSaV replication. PSaV-infected cells maintained low levels of NO prior to 36 hpi, when a significant increase in PGE₂ production was observed (Fig. 8A). These data suggested that COX induction and the associated increase in PGE₂ production may play important roles in the inhibition of NO production during PSaV replication.

To examine this possibility further, the effect of the COX-2 inhibitor NS-398 on NO production during PSaV infection was also examined (Fig. 8B). Inhibition of COX-2 activity was found to lead to a concomitant increase in NO production during PSaV replication, which could be reversed in a dose-dependent manner by the addition of the nitric oxide synthase (NOS) inhibitor L-NAME (Fig. 8B). The reversal of the effect of COX-2 inhibition by L-NAME also resulted in the subsequent restoration of PSaV infectivity levels, as well as PSaV RNA and protein levels (Fig. 8C to E). Collectively, these data suggest that the proviral effects of PGE₂ produced by both the COX-1 and COX-2 enzymes as a result of PSaV infection are mediated by the inhibition of the antiviral effect of NO.

DISCUSSION

During viral infection, numerous host inflammatory responses are induced, leading to the production of cellular effectors and soluble factors, such as IFNs, PGE₂, and NO (21, 22). As obligate intracellular parasites, viruses must therefore subvert and/or avoid the host response to infection in order to complete their life cycle. As a result, pathogens, including viruses, have evolved a wide variety of mechanisms that enable the control of cellular pathways, evade the host immune response, and hijack signaling pathways to facilitate viral replication and pathogenesis. Here, we investigated the

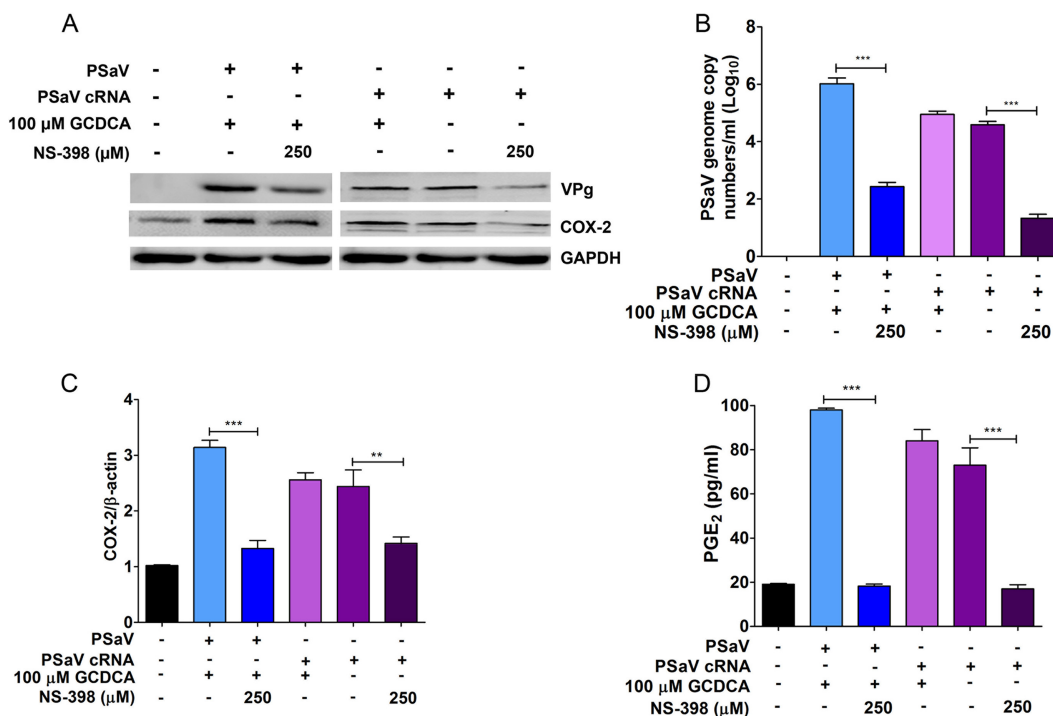


FIG 6 Bile acid GCDCA does not influence the expression of COX-2 during PSaV infection. (A to C) LLC-PK cells were either infected with PSaV (MOI = 1 FFU/cell) or transfected with 1 μg of *in vitro*-transcribed PSaV-capped RNA, and the effect of the COX-2 inhibitor NS-398 or the bile acid GCDCA was examined. Infected cells were harvested at 36 h postinfection, whereas transfected cells were harvested after 6 days posttransfection and subjected to Western blot analysis to assess viral protein production (A), as well as to qPCR for viral RNA (B) and COX-2 (C). (D) Supernatants were also collected for ELISA to quantify the levels of PGE₂. The data are represented as means and standard errors of the mean from the results of three independent experiments. Differences were evaluated using one-way ANOVA. **, *P* < 0.001; ***, *P* < 0.001.

potential role of the COX/PGE₂ pathway in the PSaV life cycle and the control of infection. We found that the COX/PGE₂ pathway was activated during the PSaV life cycle and that this activation had proviral effects via the inhibition of NO production. Furthermore, we determined that expression of the VPg and ProPol proteins of PSaV was sufficient to induce COX expression and PGE₂ production.

Among the soluble factors produced during the response of host cells to viral infection, NO is well known in the antiviral repertoire (23–26). In the immunological system, inducible NOS (iNOS) is induced by cytokines at the transcriptional level primarily in macrophages, neutrophils, epithelial cells, and hepatocytes, where NO is produced at high concentrations (27, 28). iNOS, the enzyme responsible for the production of NO, can be regulated by the COX/PGE₂ pathway (25). NO production is known to restrict vesicular stomatitis virus (VSV) infection (23), an effect that is thought to be offset by the induction of PGE₂ production during VSV replication *in vivo* (18). Here, we showed that activation of the COX-2/PGE₂ pathway also enhances PSaV replication through an inhibitory effect on NO production.

NO production is significantly enhanced in patients suffering from gastroenteritis (24), and this has been observed in norovirus and rotavirus infections in children (26). NO secretion can be triggered *in vitro* and *in vivo* by rotavirus nonstructural protein 4 (NSP4) (28–30), which in turn may cause diarrhea by elevating intestinal permeability (31, 32) and regulating intestinal motility (33) and intestinal ion transport (34, 35). In contrast to rotavirus infection (28–30), little NO production was observed during PSaV replication in LLC-PK cells, possibly due to the synthesis of PGE₂, suggesting that NO may not be involved in sapovirus-induced diarrhea. However, it is important to note that we cannot fully rule out a potential role for NO in PSaV pathogenesis *in vivo*, where the cellular response to infection is influenced by numerous cell types and may not be entirely reproduced in immortalized cells *in vitro*.

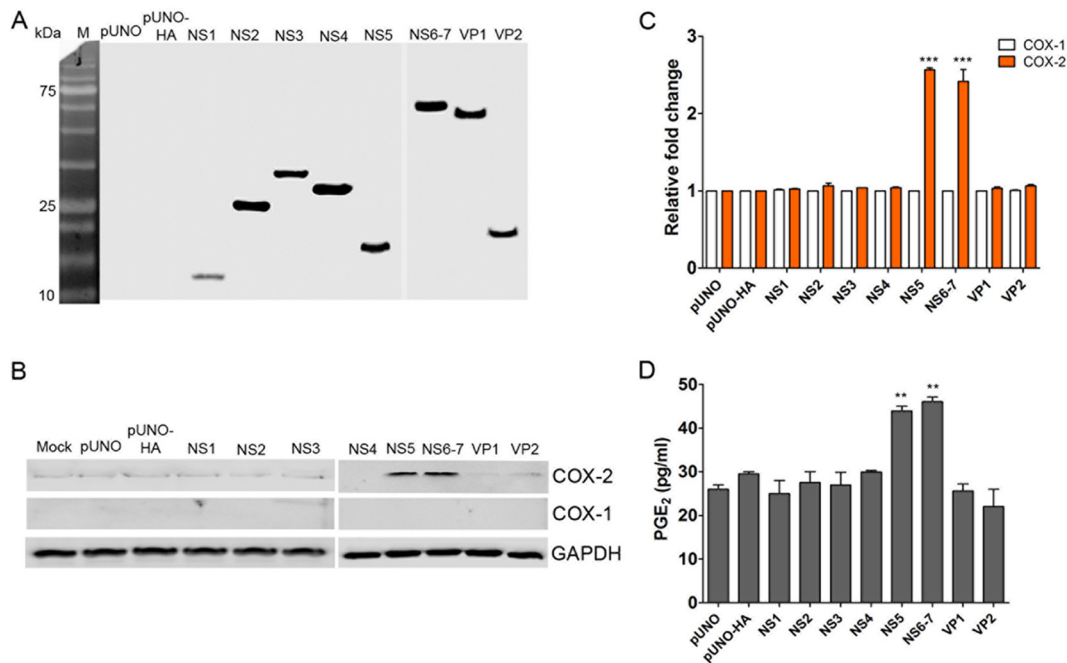


FIG 7 Role of PSaV proteins in stimulating COX-2 expression. (A and B) LLC-PK cells were transfected with 1 μ g of pUNO plasmids containing each PSaV gene tagged with an HA epitope, as indicated in Materials and Methods. As controls, pUNO empty or HA-carrying (pUNO-HA) plasmids were transfected. At 36 h posttransfection (hpt), cells were harvested, and the expression levels of viral proteins (A), as well as COX-1 and COX-2 proteins (B), were determined by Western blotting. GAPDH was used as a loading control. (C) In the cases of COX-1 and COX-2, the expression levels were also quantified by real-time PCR and normalized to β -actin and are depicted as the fold induction compared with that of vehicle-transfected cells. (D) To determine the PGE₂ concentration, supernatants were collected and ELISA was conducted. The levels of PGE₂ in the supernatants were compared between vehicle- and PSaV gene-transfected groups. The data are presented as means and standard errors of the mean from three independent experiments. Differences were evaluated using one-way ANOVA. **, $P < 0.001$; ***, $P < 0.0001$.

In a few instances, viral proteins have been shown to stimulate activation of the COX/PGE₂ pathway, often by acting either directly or indirectly as a transcriptional transactivator of COX-2 gene expression (36–39). Among the viral proteins for which this activity has been reported, the hepatitis C virus (HCV) protein NS3, a viral serine protease, is known to enhance the COX-2/PGE₂ pathway by activating multiple signaling pathways (40). In addition, the severe acute respiratory syndrome coronavirus (SARS-CoV) nucleocapsid protein also activates the expression of the COX-2/PGE₂ pathway by binding directly to regulatory elements for NF- κ B and CCAAT/enhancer binding protein (39). In the present study, we demonstrated that expression of the PSaV VPg or ProPol protein in isolation was sufficient to lead to activation of the COX-2/PGE₂ pathway. The mechanism behind this activation remains to be determined and is the subject of future study.

In the present study, the levels of COX-1/2 mRNA and proteins were increased in response to PSaV infection, so we evaluated the effects of COX-1-specific, COX-2-specific, and nonselective COX-1/2 inhibitors on PSaV replication. Among the inhibitors tested, the COX-2-specific inhibitors NS-398 and celecoxib and the nonselective COX-1/2 inhibitor indomethacin exerted stronger anti-PSaV effects than other inhibitors, with \sim 1,000-fold decreases in virus yield and RNA synthesis. However, other COX-2-specific inhibitors had weaker inhibitory effects on PSaV replication, most likely due to their less potent activity and the fact that higher concentrations required for effective COX inhibition resulted in cell toxicity observed during their use. In addition, more robust inhibitory effects of the COX-2-specific inhibitor NS-398 and the COX-1/2 nonselective inhibitor indomethacin on PSaV replication was observed in posttreatment than in pre/posttreatment. The reason why posttreatment with these inhibitors has a stronger effect than pre/posttreatment remains unknown. One possibility is that

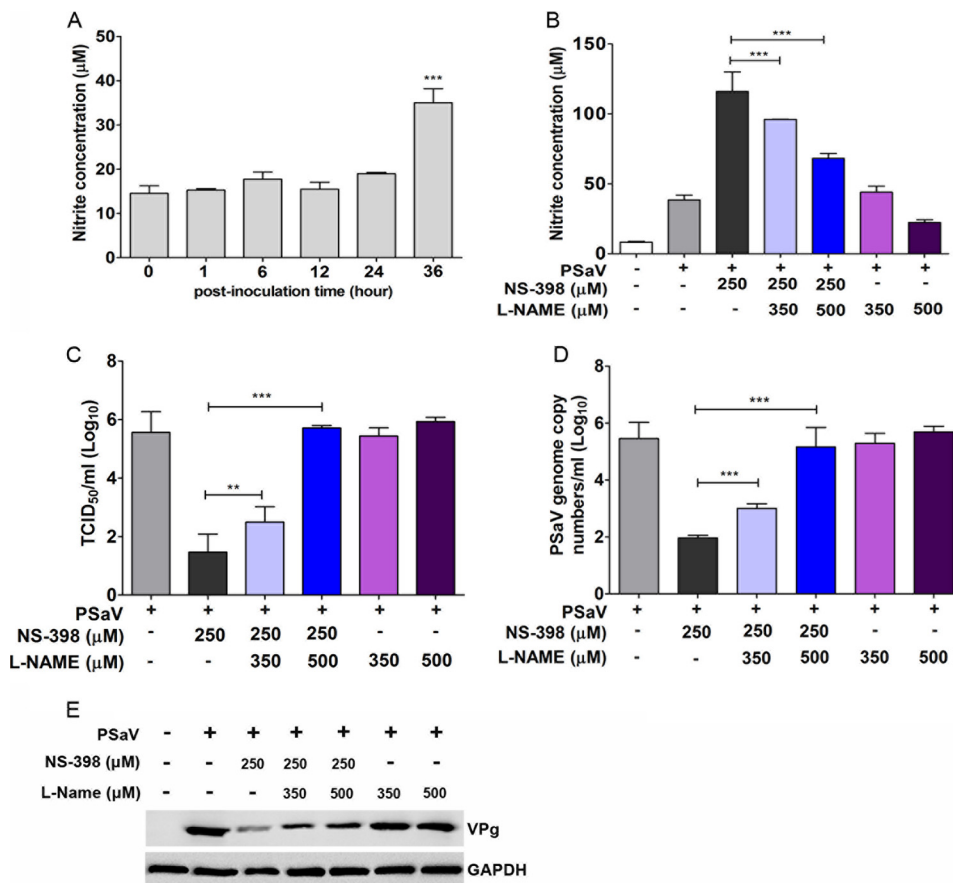


FIG 8 PGE₂ blocks the antiviral effect of nitric oxide on PSaV infection. (A) Supernatants from mock- or PSaV-infected samples were collected, and the nitrite concentration was determined using the Griess reagent system, as described in Materials and Methods. LLC-PK cells were infected with PSaV (MOI = 1 FFU/cell) and subsequently treated with the COX-2 inhibitor NS-398 or the nitric oxide synthase inhibitor L-NAME, either singly or in combination. (B) The effect of inhibitor treatment on nitric oxide production was then determined as described for panel A. (C to E) The levels of viral titer (C), RNA (D), and protein (E) were determined by TCID₅₀, real-time reverse transcription (RT)-PCR, and Western blot analyses, respectively. GAPDH served as the loading control. The data are means and standard errors of the mean from the results of three different independent experiments. Differences were evaluated by one-way ANOVA. **, *P* < 0.001; ***, *P* < 0.0001.

it could be an off-target effect of using high doses of the inhibitors in LLC-PK cells, although there are no published reports of these kinds of phenomena.

In the present study, we observed only a transient increase in COX-1 levels during PSaV infection, whereas COX-2 induction was more significantly induced and the induction was sustained during the later stage of the viral life cycle. However, the dramatic effects of the nonselective COX inhibitor indomethacin, the COX-2-specific inhibitor NS-398, and the COX-specific siRNAs support the hypothesis that both the COX-1 and COX-2 enzymes play roles in PSaV replication.

In conclusion, our results demonstrate a crucial role of the COX/PGE₂ pathway in the regulation of NO production during PSaV replication, which provides an environment suitable for efficient PSaV growth. In addition, our data indicate that pharmacological targeting of COX-2 could provide a potential targeting strategy for the control of sapovirus infection, facilitating the antiviral effect of NO production. Further studies are required to determine if targeting the COX/PGE₂ pathway *in vivo* has a negative impact on PSaV pathogenesis.

MATERIALS AND METHODS

Cells and virus. LLC-PK porcine kidney cells obtained from the American Type Culture Collection (ATCC) were maintained in Eagle’s minimal essential medium (EMEM) containing 10% fetal bovine serum (FBS), 100 U/ml penicillin, and 100 µg/ml streptomycin. The tissue culture-adapted PSaV strain Cowden

was recovered from the full-length infectious clone pCV4A and was propagated in LLC-PK cells supplemented with bile acid (15).

Chemicals and antibodies. Celecoxib, NS-398, SC-58125, SC-236, nimesulide, and SC-560 were purchased from Cayman Chemical (Ann Arbor, MI, USA). GCDCA, dimethyl sulfoxide (DMSO), L-NAME, MDL-12330A, and indomethacin were from Sigma-Aldrich (St. Louis, MO, USA). COX-1 siRNA, COX-2 siRNA, and scrambled siRNA were purchased from Santa Cruz Biotechnology, Inc. (Santa Cruz, CA, USA). Monoclonal antibody (MAb) against mouse COX-1 and polyclonal antibody against rabbit COX-2 were obtained from Abcam (Cambridge, MA, USA). Mouse MAb against HA tag was purchased from OriGene (Rockville, MD, USA). Synthetic PGE₂ was purchased from Tocris Bioscience (Ellisville, MO, USA). The anti-PSaV capsid MAb and the anti-PSaV VPg polyclonal antibody were previously described (41). The secondary antibodies used were horseradish peroxidase-conjugated goat immunoglobulin against rabbit IgG (Cell Signaling, Beverly, MA, USA) and mouse IgG (Santa Cruz) and fluorescein isothiocyanate (FITC)-conjugated goat immunoglobulin against rabbit IgG (Jackson Immuno Research Laboratory, West Grove, PA, USA).

Cytotoxicity assay. The cytotoxicity of the chemicals used in this study was determined using the 3-(4,5-dimethylthiazol-2-yl)-2,5-diphenyl tetrazolium bromide (MTT) assay (42, 43) according to the manufacturer's instructions. Briefly, cells in 96-well plates were incubated with medium containing different concentrations of various chemicals for 24 h. After removal of the medium, 200 μ l of MTT solution was added to each well and incubated for 4 h at 37°C in a CO₂ incubator. Each well was supplemented with 150 μ l of DMSO and incubated at room temperature for 10 min. The absorbance as an optical density (OD) was read in an enzyme-linked immunosorbent assay (ELISA) reader at 570 nm. The percent cell viability was calculated using the following formula: $[(OD_{\text{sample}} - OD_{\text{blank}})/(OD_{\text{control}} - OD_{\text{blank}})] \times 100$. Nontoxic concentrations of each chemical were used in the study.

Treatment of LLC-PK cells with inhibitors and chemicals. LLC-PK cells were grown in 6- or 12-well plates to attain the desired confluence. The chemicals and inhibitors were dissolved in DMSO to make a 10 mM stock concentration. When appropriate, a series of dilutions were made by diluting the appropriate volumes of chemical or inhibitor stocks in EMEM. Treatment groups were typically as follows: mock treatment, pretreatment, posttreatment, and pre/posttreatment. Confluent LLC-PK cells were pretreated with various concentrations of the inhibitors for 24 h. The cells were washed with phosphate-buffered saline (PBS) (pH 7.4) and inoculated with PSaV at a multiplicity of infection (MOI) of 1 fluorescent focus unit (FFU)/cell. For posttreatment groups, different concentrations of inhibitors were added to the maintenance medium after the virus adsorption step. For the pre/posttreatment groups, LLC-PK cells were pretreated with different concentrations of inhibitors for 24 h. After the removal of the inhibitors, the cells were washed twice with PBS and inoculated with PSaV. The inhibitors were again added at the end of the virus adsorption period.

Plasmid constructs and cell culture. Each of the regions coding for the PSaV proteins NS1, NS2, NS3, NS4, NS5, NS6-7, VP1, and VP2 (17) was amplified from the full-length infectious clone pCV4A by PCR assays with primer pairs containing Sall and NheI restriction enzyme sites (Table 1). Each forward primer specific for the above-mentioned genes had N-terminal HA tag sequences (Table 1). Each amplicon was purified with PuriGel (Invitrogen, Waltham, MA, USA) following the manufacturer's instructions and subcloned into the pUNO cloning vector (Invitrogen, San Diego, CA, USA). All the amplified regions were verified by Sanger sequencing. LLC-PK cells grown in 6-well plates were individually transfected with plasmid constructs with different viral genes inserted or empty vectors using the Lipofectamine 2000 reagent (Invitrogen) following the manufacturer's instructions. Cells were harvested at different post-transfection points and subjected to quantitative real-time PCR and Western blot analysis using the anti-HA antibody.

In vitro transcription and RNA transfection. LLC-PK cells were seeded in 6-well or 24-well plates and transfected with 1 μ g of capped *in vitro*-transcribed PSaV RNA using Lipofectamine 2000 (Invitrogen). The capped *in vitro* transcripts were derived from the full-length PSaV cDNA clone pCV4A (44) with the mMessage mMachine kit (Ambion, Austin, TX, USA) following the manufacturer's instructions. Transfections were performed for 4 h, and the medium was replenished with EMEM supplemented or not with 200 μ M GCDCA. Six days posttransfection, the cells were lysed, harvested, and subjected to immunoblotting and qPCR to analyze COX-1, COX-2, and PSaV VPg levels.

siRNA transfection. LLC-PK cells were cultured in 6- or 12-well culture plates at 70 to 80% confluence and transfected with siRNA (80 pmol of COX-1, COX-2, and scrambled control siRNA) using the Lipofectamine 2000 reagent (Invitrogen) following the manufacturer's instructions. The cells were then infected with PSaV at an MOI of 1 FFU/cell. After 1 h, unadsorbed viruses were removed and the cells were maintained in EMEM with 2.5% FBS and 100 μ M GCDCA. Cells were harvested at different time points and subjected to qPCR and median (50%) tissue culture infective dose (TCID₅₀) and Western blot analyses.

Preparation of cell extracts and Western blot analysis. Confluent LLC-PK cells in 6-well plates infected or not with PSaV, treated or not with chemicals or inhibitors, transfected or not with siRNAs, or transfected or not with each gene construct of PSaV were harvested at different time points. The cells were washed twice with PBS and lysed with a cell extraction buffer (Invitrogen) supplemented with protease and phosphatase inhibitors (Roche, Basel, Switzerland). Total cell lysates were denatured and resolved in sodium dodecyl sulfate (SDS)-polyacrylamide gels. The resolved proteins were transferred to nitrocellulose blotting membranes (Amersham Protran; GE Healthcare Life Science, Germany) and immunoblotted with primary antibodies specific for COX-1, COX-2, glyceraldehyde 3-phosphate dehydrogenase (GAPDH), HA, or PSaV VPg. Secondary antibodies against rabbit or mouse IgG were applied after the primary antibody. Immunoreactive bands were developed using an enhanced chemilumines-

TABLE 1 Oligonucleotide primers used in the study

| Target gene | Primer name | Orientation ^a | Sequence (5'–3') ^b | Region (nt) ^e | Size (bp) |
|--------------------|----------------|--------------------------|---|--------------------------|-----------|
| p11 | pUNO-HA-p11 | F | gtg <u>gtcgac</u> atg TAC CCA TAC GAT GTT CCA GAT TAC GCT GCT AAT TGC CGT CCG TTG CCT ATT GGG | 13–39 | 165 |
| | | R | atc <u>gctagc</u> TCA TTG CGC CAC AAA CAC GTC | | |
| p28 | pUNO-HA-p28 | F | ttt <u>gtcgac</u> atg TAC CCA TAC GAT GTT CCA GAT TAC GCT GGG GTG GTG GAT GAT TTC TTC CGC CCC | 177–160 | 762 |
| | | R | atc <u>gctagc</u> TCA CTG CGG CGT GTA GAG GC | 939–923 | |
| p35 | pUNO-HA-p35 | F | tac <u>gtcgac</u> atg TAC CCA TAC GAT GTT CCA GAT TAC GCT GCA GGC AAT GAT CTC ATC ATA TTG GGG | 940–966 | 1,017 |
| | | R | gac <u>gctagc</u> TCA CTC GCT GTT GTA CTT C | 1956–1941 | |
| p32 | pUNO-HA-p32 | F | tac <u>gtcgac</u> atg TAC CCA TAC GAT GTT CCA GAT TAC GCT GCC GCT GAT GTC AAA CAT CTA TGG TTC | 1957–1983 | 855 |
| | | R | ttt <u>gctagc</u> TCA CTC GCT AAG CGT GTT TTC | 2811–2794 | |
| VPg | pUNO-HA-VPg | F | ac <u>gtcgac</u> atg TAC CCA TAC GAT GTT CCA GAT TAC GCT GCG AAA GGG AAA AAC AAA CGC GGA CGT | 2812–2838 | 338 |
| | | R | <u>gctagc</u> TCA CTC ACT GTC ATA GGT GTC ACC TTT | 3150–3133 | |
| ProPol | pUNO-HA-ProPol | F | <u>gtcgac</u> atg TAC CCA TAC GAT GTT CCA GAT TAC GCT GGG CGT GGA TAC GTG GTA CCC ATG AC | 3151–3177 | 1,995 |
| | | R | <u>gctagc</u> TCA CTC ACT GTC ATA GGT GTC ACC TTT | 5145–5128 | |
| VP1 | pUNO-HA-VP1 | F | <u>gtcgac</u> atg TAC CCA TAC GAT GTT CCA GAT TAC GCT GAG GCG CCT GCC CCA ACC CGT TCG GTT | 5144–5169 | 1,627 |
| | | R | <u>gctagc</u> TCATCGTGAGCTGTGAATGGACCTTCC | 6771–6753 | |
| VP2 | pUNO-HA-VP2 | F | ctc <u>gtcgac</u> atg TAC CCA TAC GAT GTT CCA GAT TAC GCT AGT TGG ATT GCA GGA GCA ATG CAG GGC | 6774–6800 | 492 |
| | | R | agg <u>gctagc</u> TCA TCA CAC TTT GCT GTG AGT G | 7265–7247 | |
| VPg | | F | CAA ACG CGG ACG TGG TGC TCG | 2826–2846 | 145 |
| | | R | TGA TGC GCC TGA CAG TGC GCG | 2970–2950 | |
| COX-1 ^c | | F | CCG GAG GAA GTT CAT ACC TGA CCC | 253–275 | 108 |
| | | R | GCC AGG ACC CAT CTT GCC AGA | 360–340 | |
| COX-2 ^d | | F | CAC CCA TGG GTG TGA AAG GGA GG | 181–203 | 201 |
| | | R | CCA AAG GAC AGG GCC ATG GGG | 381–361 | |

^aF, forward; R, reverse.

^bLowercase underlined letters, restriction enzyme sites (forward primers, Sall; reverse primers, NheI); italic letters, polypeptide hemagglutinin sequences; lowercase boldface letters, start codons. The lowercase letters at the start of the forward primers of the PSaV genome are overhang sequences.

^cDerived from partial sequence of porcine COX-1 (GenBank accession no. AF207823.1).

^dDerived from partial sequence of porcine COX-2 (GenBank accession no. AF207824.1).

^ent, nucleotides.

cence reaction kit (DoGen, Seoul, South Korea), and images were taken using the Davinch-Western imaging system (Young Ltd., Kang-Nam, Seoul, South Korea). To confirm equal protein loading, the blotting membranes were also incubated with an antibody against GAPDH, and its reactivity was compared with the intensities of target bands. The quantification of the protein densities for COX-1 and COX-2 was performed using Image Studio Lite (LI-COR Biotechnology, Lincoln, NE, USA) and was normalized to the corresponding density of GAPDH in the same samples.

RNA isolation. To quantify intracellular RNA levels of signaling molecules, mock- or PSaV-infected, chemical- or inhibitor-treated, or siRNA-transfected cells were washed twice with PBS, scraped, and collected in clean microtubes. Samples were centrifuged at 10,000 rpm for 10 min, and total RNA was isolated using the PureLink RNA minikit (Ambion Life Technologies, Carlsbad, CA, USA) following the manufacturer's instructions. To quantify PSaV RNA, mock- or PSaV-infected, chemical- or inhibitor-treated, or siRNA-transfected cells were freeze-thawed three times, and the cell debris was spun down at $2,469 \times g$ for 10 min at 4°C. The supernatants, along with the remaining bulk samples, were collected and stored at –80°C until they were used. Total RNA was extracted from supernatants using an RNeasy kit (Qiagen) following the manufacturer's instructions. The RNA concentrations were spectrophotometrically determined at 260 nm using a BioPhotometer plus (Eppendorf, Hamburg, Germany).

Quantitative real-time PCR. cDNAs were prepared by using 1 μg of RNA and reverse transcribed using random hexamers (Promega, Madison, WI, USA). The oligonucleotide primers used in the quantitative real-time PCR were designed from the published sequences of COX-1, COX-2, and PSaV VPg (Table 1). Reaction mixtures were set up in 25-μl volumes containing 10 pmol of forward and reverse primers, cDNA, and Topreal qPCR 2× premix (Enzynomics, Daejeon, South Korea). For COX-1 and COX-2, the amplification profile was as follows: 1 cycle of initial denaturation at 95°C for 10 min and 45 cycles of denaturation at 95°C for 10 s, primer annealing at 55°C for 30 s, and extension at 72°C for 45 s. The amplification profile for VPg included denaturation at 95°C for 10 min, followed by 40 cycles of denaturation at 95°C for 10 s, primer annealing at 60°C for 20 s, and extension at 72°C for 20 s. Relative COX-1 and COX-2 expression levels were calculated using $2^{-\Delta\Delta CT}$ (45). Samples were normalized to the quantity of β-actin genes. The copy number of the VPg gene was calculated using 10-fold dilutions of a known amount of pCV4A to generate the standard curve.

TCID₅₀ assay. The TCID₅₀ assay was performed as previously described (6). Briefly, 10-fold serial dilutions of clarified virus supernatants were prepared in EMEM. Of these dilutions, 200 μl was inoculated into monolayers of LLC-PK cells grown on 96-well plates supplemented with 200 μM GCDCA and incubated at 37°C in a 5% CO₂ incubator. Virus titers were calculated at 6 days postinfection and expressed as TCID₅₀/ml values by the method of Reed and Muench (46).

Determination of infectivity titers by immunofluorescence assay. Infectivity assays were carried out as described previously (41). Briefly, confluent monolayers of cells on a confocal dish were treated with various inhibitors or chemicals as described above. Mock-treated or inhibitor-treated cells were infected with PSaV at an MOI of 1 FFU/cell and incubated at 37°C for 1 h. The cells were washed three times with PBS, moved to maintenance medium, and then incubated for 36 h at 37°C prior to being fixed with 4% formaldehyde in PBS.

Immunofluorescence assays were performed as previously reported (41). Briefly, fixed cells in 8-well chamber slides were permeabilized by the addition of 0.2% Triton X-100, incubated at room temperature for 10 min, and washed with PBS containing 0.1% newborn calf serum (PBS-NCS). The chamber slides were supplemented with anti-PSaV capsid (1:40 dilution) MAbs and then incubated at 4°C overnight. The cells were then washed three times with PBS-NCS, and FITC-conjugated goat secondary antibody (diluted 1:100) was added. After washing with PBS, the chambers were mounted with SlowFade Gold antifade reagent (Life Technologies, Eugene, OR, USA) containing DAPI (4',6-diamidino-2-phenylindole) solution for nuclear staining. Infected cells were observed with an LSM 510 confocal microscope and analyzed using LSM software (Carl Zeiss). To calculate the percentages of antigen-positive cells, 1,000 cells in each well were counted using a 40× objective and a 10× eyepiece, yielding a final magnification of ×400. The numbers of antigen-positive cells in mock- and drug-treated or scrambled RNA and siRNA against the COX-2 gene were compared.

Determination of NO concentrations. The concentrations of NO in culture supernatants of mock- or PSaV-infected cells in the presence or absence of chemicals or inhibitors were determined by assaying nitrite, one of its stable end products. The collected supernatants were centrifuged to remove cell debris. The assay was done using the Griess reagent system (Promega, Madison, WI, USA) according to the manufacturer's instructions. Briefly, equal volumes of each experimental sample and sulfanilamide solution were incubated at room temperature for 10 min. An equal volume of *N*-1-naphthylethylenediamine dihydrochloride solution was then added to all the wells and incubated for 10 min. The absorbance was read at 540 nm in a plate reader. The nitrite concentration of each sample was determined by comparing it with a generated nitrite standard and calculated by linear regression analysis.

ACKNOWLEDGMENTS

We thank Kyeong-Ok Chang (Kansas State University) for his generous gift of the full-length infectious clone pCV4A.

The study was supported by a grant (2014R1A2A2A01004292) from the Basic Science Research Program through the National Research Foundation of Korea (NRF) funded by the Ministry of Science, ICT and Future Planning; a Korea Basic Science Institute grant (C33730); and the Bio-Industry Technology Development Program (315021-04) funded by the Ministry of Agriculture, Food and Rural Affairs, Republic of Korea. I.G. is a Wellcome Senior Fellow supported by the Wellcome Trust (097997/Z/11/Z).

REFERENCES

- Anderson EJ. 2010. Prevention and treatment of viral diarrhea in pediatrics. *Expert Rev Anti Infect Ther* 8:205–217. <https://doi.org/10.1586/eri.10.1>.
- Ayukekbong JA, Mesumbe HN, Oyero OG, Lindh M, Berdström T. 2015. Role of noroviruses as aetiological of diarrhea in developing countries. *J Gen Virol* 96:1983–1999. <https://doi.org/10.1099/vir.0.000194>.
- Patel MM, Hall AJ, Vinjé J, Parashar UD. 2009. Noroviruses: a comprehensive review. *J Clin Virol* 44:1–8. <https://doi.org/10.1016/j.jcv.2008.10.009>.
- Jones MK, Watanabe M, Zhu S, Graves CL, Keyes LR, Grau KR, Gonzalez-Hernandez MB, Iovine NM, Wobus CE, Vinjé J, Tibbetts SA, Wallet SM, Karst SM. 2014. Enteric bacteria promote human and mouse norovirus infection of B cells. *Science* 346:755–759. <https://doi.org/10.1126/science.1257147>.
- Oka T, Wang Q, Katamayan K, Saif LJ. 2015. Comprehensive review of human sapoviruses. *Clin Microbiol Rev* 28:32–53. <https://doi.org/10.1128/CMR.00011-14>.
- Hosmillo M, Sorgeloos F, Hiraide R, Lu J, Goodfellow I, Cho KO. 2015. Porcine sapovirus replication is restricted by the type I interferon response in cell culture. *J Gen Virol* 96:74–84. <https://doi.org/10.1099/vir.0.071365-0>.
- Paul AG, Chandran B, Sharma-Walia N. 2013. Cyclooxygenase-2 prostaglandin E2-eicosanoid receptor inflammatory axis: a key player in Kaposi's sarcoma-associated herpes virus associated malignancies. *Transl Res* 162:77–92. <https://doi.org/10.1016/j.trsl.2013.03.004>.
- Hooks JJ, Chin MS, Srinivasan K, Momma Y, Hoop LC, Nagineni CN, Chan CC, Detrick B. 2006. Human cytomegalovirus induced cyclooxygenase-2 in human retinal pigment epithelial cells augments viral replication through a prostaglandin pathway. *Microbes Infect* 8:2236–2244. <https://doi.org/10.1016/j.micinf.2006.04.010>.
- Zhu H, Cong JP, Yu D, Bresnahan WA, Shenk TE. 2002. Inhibition of cyclooxygenase 2 blocks human cytomegalovirus replication. *Proc Natl Acad Sci U S A* 99:3932–3937. <https://doi.org/10.1073/pnas.052713799>.
- Luczak M, Gumulka W, Szmigielski S, Korbecki M. 1975. Inhibition of multiplication of parainfluenza 3 virus in prostaglandin-treated WISH cells. *Arch Virol* 49:377–380. <https://doi.org/10.1007/BF01318248>.
- Ongrádi J, Telekes A, Farkas J, Nász I, Bendinelli M. 1994. The effect of prostaglandins on the replication of adenovirus wild types and temperature-sensitive mutants. *Acta Microbiol Immunol Hung* 41: 173–188.
- Warner TD, Mitchell JA. 2002. Cyclooxygenase-3 (COX-3): filling in the gaps toward a COX continuum? *Proc Natl Acad Sci U S A* 99: 13371–13373. <https://doi.org/10.1073/pnas.222543099>.
- Smith WL, DeWitt DL, Garavito RM. 2000. Cyclooxygenases: structural,

- cellular, and molecular biology. *Annu Rev Biochem* 69:145–182. <https://doi.org/10.1146/annurev.biochem.69.1.145>.
14. Kalinski P. 2012. Regulation of immune responses by prostaglandin E2. *J Immunol* 188:21–28. <https://doi.org/10.4049/jimmunol.1101029>.
 15. Chang KO, Sosnovtsev SV, Belliot G, Kim Y, Saif LJ, Green KY. 2004. Bile acids are essential for porcine enteric calicivirus replication in association with down-regulation of signal transducer and activator of transcription 1. *Proc Natl Acad Sci U S A* 101:8733–8738. <https://doi.org/10.1073/pnas.0401126101>.
 16. Shivanna V, Kim Y, Chang KO. 2014. The crucial role of bile acids in the entry of porcine enteric calicivirus. *Virology* 456–457:268–278. <https://doi.org/10.1016/j.virol.2014.04.002>.
 17. Oka T, Katayama K, Ogawa S, Hansman GS, Kageyama T, Ushijima H, Miyamura T, Takeda N. 2005. Proteolytic processing of sapovirus ORF1 polyprotein. *J Virol* 79:7283–7290. <https://doi.org/10.1128/JVI.79.12.7283-7290.2005>.
 18. Chen N, Warner JL, Shoshkes-Reiss C. 2000. NSAID treatment suppresses VSV propagation in mouse CNS. *Virology* 276:44–51. <https://doi.org/10.1006/viro.2000.0562>.
 19. Akaike T, Maeda H. 2000. Nitric oxide and virus infection. *Immunology* 101:300–308. <https://doi.org/10.1046/j.1365-2567.2000.00142.x>.
 20. Guzik TJ, Korbut R, Adamek-Guzik T. 2003. Nitric oxide and superoxide in inflammation and immune function. *J Physiol Pharmacol* 54:469–487.
 21. Steer S, Corbett JA. 2003. The role and regulation of COX-2 during viral infection. *Viral Immunol* 16:447–460. <https://doi.org/10.1089/088282403771926283>.
 22. Koyama S, Ishii KJ, Coban C, Akira S. 2008. Innate immune response to viral infection. *Cytokine* 43:336–341. <https://doi.org/10.1016/j.cyto.2008.07.009>.
 23. Bi Z, Reiss CS. 1995. Inhibition of vesicular stomatitis virus infection by nitric oxide. *J Virol* 69:2208–2213.
 24. Herulf M, Svenungsson B, Lagergren A, Ljung T, Morcos E, Wiklund NP, Lundberg JO, Weitzberg E. 1999. Increased nitric oxide in infective gastroenteritis. *J Infect Dis* 180:542–545. <https://doi.org/10.1086/314908>.
 25. Kash JC, Goodman AG, Korth MJ, Katze MG. 2006. Hijacking of the host-cell response and translational control during influenza virus infection. *Virus Res* 119:111–120. <https://doi.org/10.1016/j.virusres.2005.10.013>.
 26. Sowmyanarayanan TV, Natarajan SK, Ramachandran A, Sarkar R, Moses PD, Simon A, Agarwal I, Christopher S, Kang G. 2009. Nitric oxide production in acute gastroenteritis in Indian children. *Trans R Soc Trop Med Hyg* 103:849–851. <https://doi.org/10.1016/j.trstmh.2009.05.003>.
 27. Zaki MH, Akuta T, Akaike T. 2005. Nitric oxide-induced nitrate stress involved in microbial pathogenesis. *J Pharmacol Sci* 98:117–129. <https://doi.org/10.1254/jphs.CRJ05004X>.
 28. Rodríguez-Díaz J, Banasaz M, Istrate C, Buesa J, Lundgren O, Espinoza F, Sundqvist T, Rottenberg M, Svensson L. 2006. Role of nitric oxide during rotavirus infection. *J Med Virol* 78:979–985. <https://doi.org/10.1002/jmv.20650>.
 29. Borghan MA, Mori Y, El-Mahmoudy AB, Ito N, Sugiyama M, Takewaki T, Minamoto N. 2007. Induction of nitric oxide synthase by rotavirus enterotoxin NSP4: implications for rotavirus pathogenicity. *J Gen Virol* 88:2064–2072. <https://doi.org/10.1099/vir.0.82618-0>.
 30. Ge Y, Mansell A, Ussher JE, Brooks AE, Manning K, Wang CJ, Taylor JA. 2013. Rotavirus NSP4 triggers secretion of proinflammatory cytokines from macrophages via Toll-like receptor 2. *J Virol* 87:11160–11167. <https://doi.org/10.1128/JVI.03099-12>.
 31. Kubes P. 1992. Nitric oxide modulates epithelial permeability in the feline small intestine. *Am J Physiol* 262:G1138–G1142.
 32. Kukuruzovic R, Robins-Browne RM, Anstey NM, Brewster DR. 2002. Enteric pathogens, intestinal permeability and nitric oxide production in acute gastroenteritis. *Pediatr Infect Dis J* 21:730–739. <https://doi.org/10.1097/00006454-200208000-00007>.
 33. Hoffman RA, Zhang G, Nüssler NC, Gleixner SL, Ford HR, Simmons RL, Watkins SC. 1997. Constitutive expression of inducible nitric oxide synthase in the mouse ileal mucosa. *Am J Physiol Gastrointest Liver Physiol* 272:G383–G392.
 34. Resta-Lenert S, Barrett KE. 2002. Enteroinvasive bacteria alter barrier and transport properties of human intestinal epithelium: role of iNOS and COX-2. *Gastroenterology* 122:1070–1087. <https://doi.org/10.1053/gast.2002.32372>.
 35. Rhee SJ, Wilson KT, Gobert AP, Nataro JP, Fasano A. 2001. The enterotoxic activity of Shigella enterotoxin 1 (ShET1) is mediated by inducible nitric oxide synthase activity. *J Pediatr Gastroenterol Nutr* 33:400–416. <https://doi.org/10.1097/00005176-200109000-00038>.
 36. Lee CH, Yeh TH, Lai HC, Wu SY, Su IJ, Takada K, Chang Y. 2011. Epstein-Barr virus Zta-induced immunomodulators from nasopharyngeal carcinoma cells upregulate interleukin-10 production from monocytes. *J Virol* 85:7333–7342. <https://doi.org/10.1128/JVI.00182-11>.
 37. Alvarez S, Serramía MJ, Fresno M, Muñoz-Fernández MA. 2007. HIV-1 envelope glycoprotein 120 induces cyclooxygenase-2 expression in astrocytoma cells through a nuclear factor-kappaB-dependent mechanism. *Neuromolecular Med* 9:179–193. <https://doi.org/10.1007/BF02685891>.
 38. Muroso S, Inoue H, Tanabe T, Joab I, Yoshizaki T, Furukawa M, Pagano JS. 2001. Induction of cyclooxygenase-2 by Epstein-Barr virus latent membrane protein 1 is involved in vascular endothelial growth factor production in nasopharyngeal carcinoma cells. *Proc Natl Acad Sci U S A* 98:6905–6910. <https://doi.org/10.1073/pnas.121016998>.
 39. Yan X, Hao Q, Mu Y, Timani KA, Ye L, Zhu Y, Wu J. 2006. Nucleocapsid protein of SARS-CoV activates the expression of cyclooxygenase-2 by binding directly to regulatory elements for nuclear factor-kappa B and CCAAT/enhancer binding protein. *Int J Biochem Cell Biol* 38:1417–1428. <https://doi.org/10.1016/j.biocel.2006.02.003>.
 40. Tomei L, Failla C, Santolini E, De Francesco R, La Monica N. 1993. NS3 is a serine protease required for processing of hepatitis C virus polyprotein. *J Virol* 67:4017–4026.
 41. Kim DS, Hosmillo M, Alfajaro MM, Kim JY, Park JG, Son KY, Ryu EH, Sorgeloos F, Kwon HJ, Park SJ, Lee WS, Cho D, Kwon J, Choi JS, Kang MI, Goodfellow I, Cho KO. 2014. Both α 2,3- and 2,6-linked sialic acids on O-linked glycoproteins act as functional receptors for porcine sapovirus. *PLoS Pathog* 10:e1004172. <https://doi.org/10.1371/journal.ppat.1004172>.
 42. Mosmann T. 1983. Rapid colorimetric assay for cellular growth and survival: application to proliferation and cytotoxicity assays. *J Immunol Methods* 65:55–63. [https://doi.org/10.1016/0022-1759\(83\)90303-4](https://doi.org/10.1016/0022-1759(83)90303-4).
 43. Kim DS, Son KY, Koo KM, Kim JY, Alfajaro MM, Park JG, Hosmillo M, Soliman M, Baek YB, Cho EH, Lee JH, Kang MI, Goodfellow I, Cho KO. 2016. Porcine sapelovirus uses α 2,3-linked sialic acid on GD1a ganglioside as a receptor. *J Virol* 90:4067–4077. <https://doi.org/10.1128/JVI.02449-15>.
 44. Chang KO, Sosnovtsev SV, Belliot G, Wang Q, Saif LJ, Green KY. 2005. Reverse genetics system for porcine enteric calicivirus, a prototype sapovirus in the Caliciviridae. *J Virol* 79:1409–1416. <https://doi.org/10.1128/JVI.79.3.1409-1416.2005>.
 45. Alfajaro MM, Kim HJ, Park JG, Ryu EH, Kim JY, Jeong YJ, Kim DS, Hosmillo M, Son KY, Lee JH, Kwon HJ, Ryu YB, Park SI, Lee WS, Cho KO. 2012. Anti-rotaviral effects of Glycyrrhiza uralensis extract in piglets with rotavirus diarrhea. *Virol J* 9:310. <https://doi.org/10.1186/1743-422X-9-310>.
 46. Reed LJ, Muench H. 1938. A simple method of estimating fifty per cent endpoints. *Am J Hyg* 27:493–497.